MOLECULAR AND CELLULAR BIOLOGY, Mar. 2009, p. 1222–1234 Vol. 29, No. 5
0270-7306/09/$08.00+0 doi:10.1128/MCB.01660-08

PTEN Loss Promotes Mitochondrially Dependent Type II Fas-Induced Apoptosis via PEA-15▽

James W. Peacock,[1,2] Jodie Palmer,[1,2] Dieter Fink,[1,2] Stephen Ip,[1,2] Eric M. Pietras,[5] Alice L.-F. Mui,[2] Stephen W. Chung,[2] Martin E. Gleave,[1,3] Michael E. Cox,[1,3] Ramon Parsons,[4] Marcus E. Peter,[5] and Christopher J. Ong[1,2]*

The Prostate Centre at Vancouver General Hospital[1] and Departments of Surgery[2] and Urological Sciences,[3] University of British Columbia, Vancouver, British Columbia V6H 3Z6, Canada; Department of Pathology and Medicine, Institute for Cancer Genetics, Columbia University, 1150 St. Nicholas Avenue, RBP 302, New York, New York[4]; and Ben May Department for Cancer, University of Chicago, Chicago, Illinois 60637[5]

Received 24 October 2008/Returned for modification 7 December 2008/Accepted 10 December 2008

Two distinct biochemical signals are delivered by the CD95/Fas death receptor. The molecular basis for the differential mitochondrially independent (type I) and mitochondrially dependent (type II) Fas apoptosis pathways is unknown. By analyzing 24 Fas-sensitive tumor lines, we now demonstrate that expression/activity of the PTEN tumor suppressor strongly correlates with the distinct Fas signals. PTEN loss-of-function and gain-of-function studies demonstrate the ability to interconvert between type I and type II Fas pathways. Importantly, from analyses of Bcl-2 transgenic *Pten*$^{+/-}$ mice, *Pten* haploinsufficiency converts Fas-induced apoptosis from a Bcl-2-independent to a Bcl-2-sensitive response in primary thymocytes and activated T lymphocytes. We further show that PTEN influences Fas signaling, at least in part, by regulating PEA-15 phosphorylation and activity that, in turn, regulate the ability of Bcl-2 to suppress Fas-induced apoptosis. Thus, PTEN is a key molecular rheostat that determines whether a cell dies by a mitochondrially independent type I versus a mitochondrially dependent type II apoptotic pathway upon Fas stimulation.

Two types of Fas apoptotic signaling pathways, designated the type I and type II pathways, occur in distinct classes of cells (2). Biochemically, type I and type II cells differ primarily in the amounts of FADD and caspase-8 recruited to the Fas receptor, in the kinetics of caspase cascade activation, and in their relative dependence on the mitochondrial intrinsic arm of the Fas apoptotic pathway in the execution of cell death (34). Fas receptor aggregation leads to the recruitment of the adaptor protein FADD and the initiator caspase-8 and -10, forming the death-inducing signaling complex (DISC) and resulting in autoproteolytic activation of these caspases. In type I cells, a sufficient amount of caspase-8 is processed to directly activate the effector caspase-3 and to execute apoptosis. While the intrinsic mitochondrial apoptotic pathway is also activated in type I cells, the relative contribution of this branch to apoptosis induction is diminished by the potent action of the direct pathway. In contrast to type I cells and despite similar expression of cell surface Fas, type II cells form a weak DISC and exhibit delayed kinetics of caspase-8 and -3 activation. Due to the paucity of FADD recruitment and caspase-8 processing at the DISC in type II cells, the direct activation of caspase-3 is attenuated, resulting in the increased dependence of type II cells on the mitochondrial amplification loop activated by the proapoptotic Bcl-2 member Bid in order to execute apoptosis. Hence, type I cells undergo Fas-mediated apoptosis in a mitochondrially independent manner, whereas type II cells have increased dependence on the intrinsic mitochondrial pathway to induce apoptosis.

Despite an intensive search, the identity of the signaling protein(s) that determines whether a cell dies by type I versus type II Fas-induced apoptosis has remained elusive (28). By virtue of their ability to regulate Fas signaling in various tissue types, a plethora of signaling proteins, including death receptor signaling proteins such as DAXX, FAP-1, FAF1, FLASH, RIP, and FLIP, apoptosis regulatory proteins such as IAP family members, Bcl-2-related proteins, and signaling proteins such as PP2A, CaMKII, PEA-15, galectin-3, PTEN, PI3K, and PKB, among others, have been implicated as potential candidates (8–11, 13–16, 21, 28, 42, 46).

In search of the signaling pathway(s) that is differentially activated in type I and type II cells, we performed a Kinetworks phosphosite screen (KPSS1.3), which simultaneously detects the presence and relative quantities of 34 critical protein phosphorylation sites, and found that the serine/threonine protein kinase B (PKB; also known as Akt) was highly phosphorylated in prototypic type II Jurkat but not type I H9 cells (Kinexus, Vancouver, BC) (data not shown). Furthermore, we noted that both of the prototypic type II cell lines, i.e., Jurkat and CEM, are known to be deficient in the PTEN tumor suppressor (33). Therefore, we hypothesized that PTEN may be an important regulator of the differential Fas signaling pathways in type I and type II cells.

The PTEN tumor suppressor gene is among the most commonly mutated genes in a broad range of human malignancies. PTEN is an important negative regulator of cell growth and survival. Among other functions, PTEN is a phosphatidylinositol 3′-phosphatase that specifically downmodulates the levels of phosphoinositide second messengers such as phosphatidyl-

* Corresponding author. Mailing address: The Prostate Centre at Vancouver General Hospital, University of British Columbia, 2660 Oak Street, Vancouver, British Columbia, Canada V6H 3Z6. Phone: (604) 875-5555, ext. 63120. Fax: (604) 875-5654. E-mail: chriso@interchange.ubc.ca.

▽ Published ahead of print on 22 December 2008.

inositol(3,4,5)-trisphosphate, thereby antagonizing the action of phosphatidylinositol 3-kinase (PI3K). Loss of PTEN function results in increased membrane phosphatidylinositol(3,4,5)-trisphosphate levels and constitutive activation of its downstream effectors, such as PKB, leading to enhanced cellular metabolism, growth, and survival (26).

In this study, we investigated whether the PI3K/PTEN pathway may be important in regulating Fas-induced apoptosis in type I and type II cells. Indeed, we found a robust correlation between PTEN expression and type I/II Fas-induced apoptosis in a wide variety of cancers. Furthermore, through PTEN gain-of-function and loss-of-function approaches, we demonstrated the ability of the PI3K/PTEN pathway to promote interconversion between the mitochondrially independent type I and mitochondrially dependent type II Fas pathways. Significantly, we found that PTEN haploinsufficiency promotes Bcl-2 sensitivity of Fas-induced apoptosis of primary thymocytes and activation-induced cell death of T lymphocytes. Furthermore, Bcl-2 sensitivity of Fas-induced apoptosis was found to be regulated by PEA-15, in a phosphorylation-dependent manner, and PEA-15 phosphorylation is mediated by the PTEN/PI3K pathway. Thus, our data indicate that the PTEN/PI3K pathway modulates the dependency of cells on the mitochondrial amplification loop to mediate Fas-induced apoptosis and determines whether a cell dies by a type I or type II Fas pathway, in part through regulating PEA-15 activity.

MATERIALS AND METHODS

Antibodies, chemicals, and reagents. Antibodies to the following proteins were used: phospho-PKB (Ser473), PKB, PTEN, poly(ADP-ribose) polymerase (PARP), human-specific cleaved PARP (Asp214), PEA-15 (Cell Signaling, Inc., Beverly, MA), and Fas (CH-11) (Immunotech, Marseille, France). Rabbit polyclonal antiactin antibody, monoclonal antivinculin (clone VIN-11-5), peroxidase-conjugated monoclonal anti-rabbit immunoglobulin G (IgG) (γ; 1:2,000), peroxidase-conjugated anti-FLAG M2 monoclonal antibody, and LY294002 were purchased from Sigma-Aldrich, Inc. (St. Louis, MO). Anti-human caspase-8 (C15) (Alexis Biochemicals), anti-human CD95 (DX2), phycoerythrin (PE)-conjugated polyclonal anti-active caspase-3, anti-cytochrome *c* monoclonal antibody (clone 7H8.2C12), anti-mouse Fas monoclonal antibody (JO2), biotinylated anti-human nerve growth factor receptor (NGFR), anti-mouse CD3ε (2C11), anti-mouse CD28 monoclonal antibody, and fluorescein isothiocyanate-conjugated anti-mouse IgG/IgM were purchased from BD Biosciences (Mississauga, Ontario, Canada). Recombinant human IgG1 Fc and Fas-Fc fusion protein were purchased from R&D Systems, Inc. (Minneapolis, MN). Soluble FasL, S2, leucine zipper-tagged FasL (LzCD95), and anti-APO-1 were provided by Marcus Peter. Anti-FADD was purchased from BD Transduction Laboratories (Lexington, KY). Rabbit anti-FADD (AB3102) polyclonal antibody was purchased from Chemicon International (Temecula, CA). Rabbit (polyclonal) anti-phospho-[Ser116]-PEA-15 antibody and horseradish peroxidase-conjugated goat $F(ab')_2$ anti-rabbit Ig were purchased from Biosource International (Camarillo, CA). PEA-15 (H-80) was purchased from Santa Cruz Biotechnology, Inc. (Santa Cruz, CA). Peroxidase-conjugated goat anti-rabbit IgG (1:2,000) was purchased from Dako Diagnostics Canada (Mississauga, Ontario, Canada), and peroxidase-conjugated goat anti-mouse IgG1 and IgG2b (1:5,000) were purchased from Southern Biotech (Birmingham, AL).

DNA cloning. The DN PTEN construct was generated using a modified lentiviral expression plasmid (FUGW) (25) where green fluorescent protein was replaced by the Gateway cassette and a blasticidin S resistance gene expression cassette was inserted downstream of the Gateway cassette (pLB-U). FLAG-tagged PTEN C124S was generated by PCR, using pcDEF FLAG-DNPTEN as the template and attB1- and attB2-containing forward (5′-GGGGACAAGTTTGTACAAAAAAGCAGGCTCCACCATGGACTACAAGGACGAC-3′) and reverse (5′-GGGGACCACTTTGTACAAGAAAGCTGGGTATCAGACTTTTGTAATTTGTGT-3′) primers, respectively, and then cloned using Invitrogen Gateway cloning technology. The final DN PTEN construct (pLB-U-DNPTEN) was confirmed by DNA sequence analysis. Lentiviral FLAG-tagged PEA-15 (pLB-U-FPEA-15WT) was derived by PCR and Gateway cloning, using the human PEA-15 cDNA clone (TC108132; OriGene Technologies, Inc., Rockville, MD) as the template and attB1- and attB2-containing forward (5′-GGGGACAAGTTTGTACAAAAAAGCAGGCTTCACCATGGATTATAAAGATGATGACGATAAAGCTGAGTACGGGACCCTCCTG-3′) and reverse (5′-GGGGACCACTTTGTACAAAGCTGGGTCTCAGGCCTTCTTCGGTGG-3′) primers, respectively. FLAG-tagged PEA-15 S116D (pLB-U-FPEA-15 S116D) was generated by site-directed mutagenesis of the human PEA-15 cDNA clone, using a QuikChange site-directed mutagenesis kit (Stratagene, La Jolla, CA) according to the manufacturer's suggested protocol, with the forward primer 5′-CATTATCCGGCAGCCCGATGAGGAAGAGATCATCAAATTGGC-3′ and reverse primer 5′-GCCAATTTGATGATCTCTTCCTCATCGGGCTGCCGGATAATG-3′, followed by Gateway cloning using the PCR primers described above. FLAG-tagged PEA-15 WT and S116G constructs containing seven silent mutations within nucleotides 221 to 255 were synthesized with flanking 5′-EcoRI-attB1 and 3′-HindIII-attB2 sites and ligated to pUC57 by Genscript Corporation (Piscataway, NJ). These FLAG-tagged PEA15 WT and S116G expression cassettes were Gateway cloned into a lentiviral expression vector (pLC-E) in which the ubiquitin promoter and the green fluorescent protein cassettes of FUGW described above were replaced with the EF1-α promoter and the cherry fluorescent protein coding sequences, respectively, to yield expression plasmids pLC-E-FPEA-15 WT (PEA-15 WT) and pLC-E-FPEA-15 S116G (PEA-15 S116G). All constructs were confirmed by DNA sequence analysis.

Generation of shRNA for PEA-15 silencing. A short hairpin RNA (shRNA) targeting PEA-15 nucleotides 221 to 250 (P221; GenBank accession number NM_0037568) was designed. RNA hairpin oligonucleotides were annealed and ligated to the BseRI and BamHI sites of pSHAG-1 (Invitrogen) to generate a PEA-15 shRNA expression gene cassette from the U6 polymerase III promoter that was then subcloned by Gateway cloning technology (Invitrogen) into the BLOCK-iT lentiviral RNA interference expression destination vector pLenti6 to generate the final expression plasmid, pLenti6 PEA-15 221. PEA-15 221 shRNA (P221)-mediated knockdown of endogenous PEA-15 was confirmed by Western blotting and quantitative real-time PCR (qPCR). Total RNA (2 μg) was reverse transcribed using the Superscript first-strand synthesis system for reverse transcription-PCR as described in the manual (Invitrogen). Synthesized cDNA (1.0 μl) was combined in a PCR with PEA-15-specific primers (forward, 5′-CTTCCTGGAGAGCCACAACAAG-3′; and reverse, 5′-GGTTAGCTTGGTGTTCCAG-3′). PEA-15 mRNA levels were normalized to the level of β-actin by using β-actin forward (5′-GCTCTTTTCCAGCCTTCCTT-3′) and reverse (5′-CGGATGTCAACGTCACACTT-3′) primers and Platinum Sybr green PCR supermix (Invitrogen). Amplification was performed on an Applied Biosystems 7900HT fast real-time PCR system. β-Actin was validated as an endogenous control for the PEA-15-specific primers, and dissociation curves resulted in a single peak of PCR amplification.

Cell lines and cell culture. Jurkat, CEM, and SKW6.4 or H9 cells (ATCC, Manassas, VA) were maintained as recommended. Jurkat-T cells were generated by stably transfecting Jurkat cells with a simian virus 40 large T antigen expression plasmid (pSV40TAg; a gift of Samuel Benchimol) and selecting transfected cells with 200 μg/ml Geneticin (G418) (Life Technologies, Gaithersburg, MD). Jurkat-T cells were used in these studies because they exhibit improved transfection efficiency (data not shown) and behave identically to parental Jurkat cells in response to Fas. Jurkat-T, Jurkat-neo, and Jurkat-Bcl-2 cells were cultured as described by Idun Pharmaceuticals, Inc. (San Diego, CA). Jurkat P221 and Jurkat-Bcl-2 P221 cells were generated by lentiviral transduction of Jurkat and Jurkat-Bcl-2 cells, respectively, with pLenti6 PEA-15 221 and subsequent selection with blasticidin (5 μg/ml). Individual clones with >70% knockdown of PEA-15 mRNA by qPCR were selected for subsequent experiments. H9-vector and H9-DN PTEN clones were generated by stable transfection with pcDEF FLAG-DN PTEN or empty vector control or by lentiviral transduction and selection with G418 (200 μg/ml) or blasticidin (3.0 μg/ml). Stable pools of H9 cells expressing vector, FPEA-15WT, or FPEA-15S116D were generated by lentivirus transduction as previously described (25), using lentiviral vector pLB-U, pLB-U-FPEA-15WT, or pLB-U-FPEA-15S116D, respectively, followed by selection with blasticidin (3 μg/ml). Jurkat P221;WT-rescue and P221;S116G cells and Jurkat-Bcl-2;P221;WT-rescue and Bcl-2;P221;S116G cells were generated by stable lentiviral transduction with either the pLC-EFPEA-15 WT or S116G vector. Populations of cells expressing the cherry fluorescent protein at >97% purity were recovered by fluorescence-activated cell sorting.

T-cell isolation. Axillary and inguinal lymph nodes and spleens were isolated from mice, followed by isolation of mononuclear cells on Lympholyte-M density separation medium (Cedarlane, Hornby, Ontario, Canada). Isolated lymphocytes were then seeded on plate-bound anti-CD3 (2C11; 2 μg/ml) and soluble anti-CD28 (2 μg/ml) (BD Biosciences, Mississauga, Canada) in 24-well plates at

a cell density of 2.0×10^6/ml in T-cell medium supplemented with 4.0 ng/ml recombinant murine interleukin-2 (IL-2) (Peprotech Canada, Inc., Ottawa, Ontario, Canada). Twenty-four hours later, the cells were cultured in T-cell medium supplemented with IL-2 for an additional 4 days. On day 4, lymphocytes were reisolated on Lympholyte-M to remove nonviable cells, washed three times in phosphate-buffered saline (PBS), and suspended in T-cell medium.

Sub-G_0/G_1 DNA content assay. Thymocytes were isolated from 3- to 4-week-old sex-matched wild-type, *Eμ-bcl-2*, *Pten*$^{+/-}$, and *Pten*$^{+/-}$; *Eμ-bcl-2* littermate mice. Thymocytes were cultured at 3.0×10^6/ml in T-cell medium (10% heat-inactivated fetal bovine serum-containing RPMI 1640 supplemented with 2 mM L-glutamine, 50 μM β-mercaptoethanol, penicillin, and streptomycin) in the absence or presence of the indicated concentration of anti-Fas antibody (JO-2). At the indicated time points, 3×10^5 (100 μl) cells were removed and diluted 10-fold in cold PBS, followed by centrifugation and fixation in 1.0 ml 80% ethanol. Fixed cells were incubated at 4°C overnight, rinsed in 1.0 ml PBS, and then washed in 1.0 ml staining buffer (PBS–0.1% Triton X-100), followed by a 30-min incubation in 0.5 ml staining buffer supplemented with RNase A (50 μg/ml) and propidium iodide (50 μg/ml) (Sigma Aldrich Inc., St. Louis, MO). The proportion of cells containing subdiploid DNA was determined by flow cytometry (Beckman-Coulter, Coulter Electronics of Canada Ltd., Burlington, Ontario, Canada). For Fas-mediated apoptosis and activation-induced cell death (AICD), T cells were suspended in medium containing IL-2 at a cell density of 3.0×10^6/ml in the presence or absence of anti-Fas (JO2) antibody, as indicated, and 24 hours later were processed for propidium iodide staining as described above.

Cell stimulation and immunoblotting. Cells were serum starved in 0.1% serum at a cell density of 5.0×10^5 cells/ml for 24 h. Viable cells were then isolated by centrifugation on Histopaque density medium (Sigma-Aldrich Inc., St. Louis, MO), plated at a density of 2.0×10^7/ml in RPMI 1640 containing 0.05% serum, and left untreated or, in some experiments, preincubated with 10 μM LY294002 or an equal volume of dimethyl sulfoxide (DMSO) (vehicle control) for 2 h at 37°C at 5% CO_2, followed by stimulation with the indicated concentration of anti-Fas antibody.

At the indicated time points, the cells were pelleted and lysed in 100 μl Nonidet P-40 lysis buffer. Lysis buffer components and immunoblotting were described previously (27), and immunoblotting used the indicated primary antibodies.

Caspase-3 assay. Jurkat-Bcl-2 or Jurkat-T cells were transfected using Lipofectamine 2000 according to the manufacturer's suggested protocol (Invitrogen Life Technologies, Burlington, Ontario, Canada). Thirty-six hours later, the cells were collected, resuspended in RPMI 1640 medium containing 0.2% fetal bovine serum, and incubated at 37°C and 5% CO_2 for 2 h, followed by treatment in the presence or absence of anti-Fas antibody (CH11; 250 ng/ml). At the indicated time points, the anti-Fas antibody was diluted 10-fold in ice-cold PBS, followed by centrifugation. Intracellular active caspase-3 assay was performed as previously described (3), and data were analyzed on an Epics XL-MCL FACScan flow cytometer (Beckman Coulter, Coulter Electronics of Canada Ltd., Burlington, Ontario, Canada). Data were analyzed using WinMDI, version 2.8, software (J. Trotter, Scripps Institute, La Jolla, CA).

DISC analysis. The amounts of DISC-associated FADD and caspase-8 were determined by immunoprecipitation as described previously (35).

Determination of mitochondrial membrane potential. To measure loss of the membrane potential ($\Delta\psi_m$), anti-Fas (CH11)- and LY294002-treated or untreated cells (5×10^5) were incubated with 460 ng/ml 3,3-dihexyloxacarbocyanine iodide [$DiOC_6(3)$], (Molecular Probes, Inc., Eugene, OR). For determination of the $\Delta\psi_m$ of transfected cells, cells were cotransfected with LSXNΔNGFR at a 1:1 molar ratio in combination with vector alone or PTEN expression plasmid. Twenty-four hours later, cells were harvested and incubated with biotinylated NGFR and purified to >90% purity, using magnetic cell sorting streptavidin-conjugated microbeads according to the manufacturer's instructions (Miltenyi Biotech, Auburn, CA). Cells were then either treated or left untreated with anti-Fas (CH11) antibody, followed by $DiOC_6(3)$ staining and FACScan analysis as described above. For loss of mitochondrial cytochrome *c*, for each treatment 2×10^7 cells were preincubated for 90 min with 10 μM LY294002, followed by stimulation in the absence or presence of anti-Fas (250 ng/ml). Mitochondrial and cytosolic fractions were isolated using a mitochondrion isolation kit for cultured cells (Pierce, Rockford, IL) according to the manufacturer's protocol.

RESULTS

PTEN expression and activity correlate with type I cells. We began our studies by examining whether PTEN expression and activity could discriminate between type I and type II cells by examining the PTEN status of the four prototypic type I (H9 and SKW6.4) and type II (Jurkat and CEM) cell lines that were used in the original study to define type I and type II cells (34). Indeed, no detectable PTEN expression and constitutive PKB phosphorylation (serine 473) were observed in type II Jurkat and CEM cells, as previously reported (33), whereas PTEN was readily detected in the type I SKW6.4 and H9 cells, with minimal steady-state PKB phosphorylation (Fig. 1A).

However, since PTEN is commonly mutated in cancer cells, it is possible that this correlation in the four prototypic cells may have occurred by chance alone. Therefore, to more rigorously test this correlation, we asked whether the association between PTEN status and type I/II phenotype would hold true for a large panel of cancer cell lines. To this end, we examined the association of PTEN protein expression and Fas type I/type II phenotypes among the wide array of tumor cell lines represented in the National Cancer Institute's chemosensitivity panel (NCI-60). The type I/type II Fas sensitivity status of the NCI-60 panel of cell lines has previously been established (1). Of 21 Fas-sensitive cell lines, 10 were type I and the remaining 11 were type II. From analyses of PTEN protein expression data available for the NCI-60 cell lines (http://dtp.nci.nih.gov/mtweb), a very strong correlation was found between PTEN protein expression and type I/II phenotypes. As shown in Table 1, 92% of type II cells expressed low levels of PTEN ($P < 0.013$), whereas 75% of type I cells highly expressed PTEN ($P < 0.017$).

Given this robust association between PTEN status and type I/II phenotype, we next examined whether PTEN plays a functional role in determining whether cells die by a type I versus a type II mechanism, using PTEN gain-of-function and loss-of-function approaches.

Conversion of type I cells to a type II-like phenotype and acquisition of sensitivity to S2-mediated cytotoxicity by expression of dominant-negative PTEN. To examine whether PTEN inhibition could convert PTEN-positive type I cells to a type II-like phenotype, we generated stable clones of type I H9 cells overexpressing a catalytically inactive PTEN C124S mutant carrying a cysteine-to-serine substitution at position 124 (DN PTEN) and functioning as a dominant inhibitor of PTEN (45) and examined whether PTEN inactivation could induce type I cells to undergo a transition toward a type II-like phenotype by monitoring three well-characterized parameters that discriminate between type I and type II cells, namely, kinetics of caspase activation, DISC formation, and S2 sensitivity.

As predicted, H9-DN PTEN cells exhibited elevated PKB phosphorylation compared to empty vector-transfected controls (H9-neo) (Fig. 1B). Type II cells display delayed kinetics of Fas-induced caspase activation compared to type I cells (34). To determine whether expression of DN PTEN in type I cells could delay Fas signaling to type II-like kinetics of Fas signaling, a time course experiment examining the kinetics of PARP cleavage was performed. Anti-Fas antibody treatment of H9-DN PTEN cells resulted in a pronounced delay of PARP cleavage compared to that in H9-neo cells (Fig. 1C), despite equivalent levels of expression of cell surface Fas (Fig. 1D). Thus, functional inactivation of PTEN promotes conversion of type I H9 cells to undergo type II-like delayed kinetics of

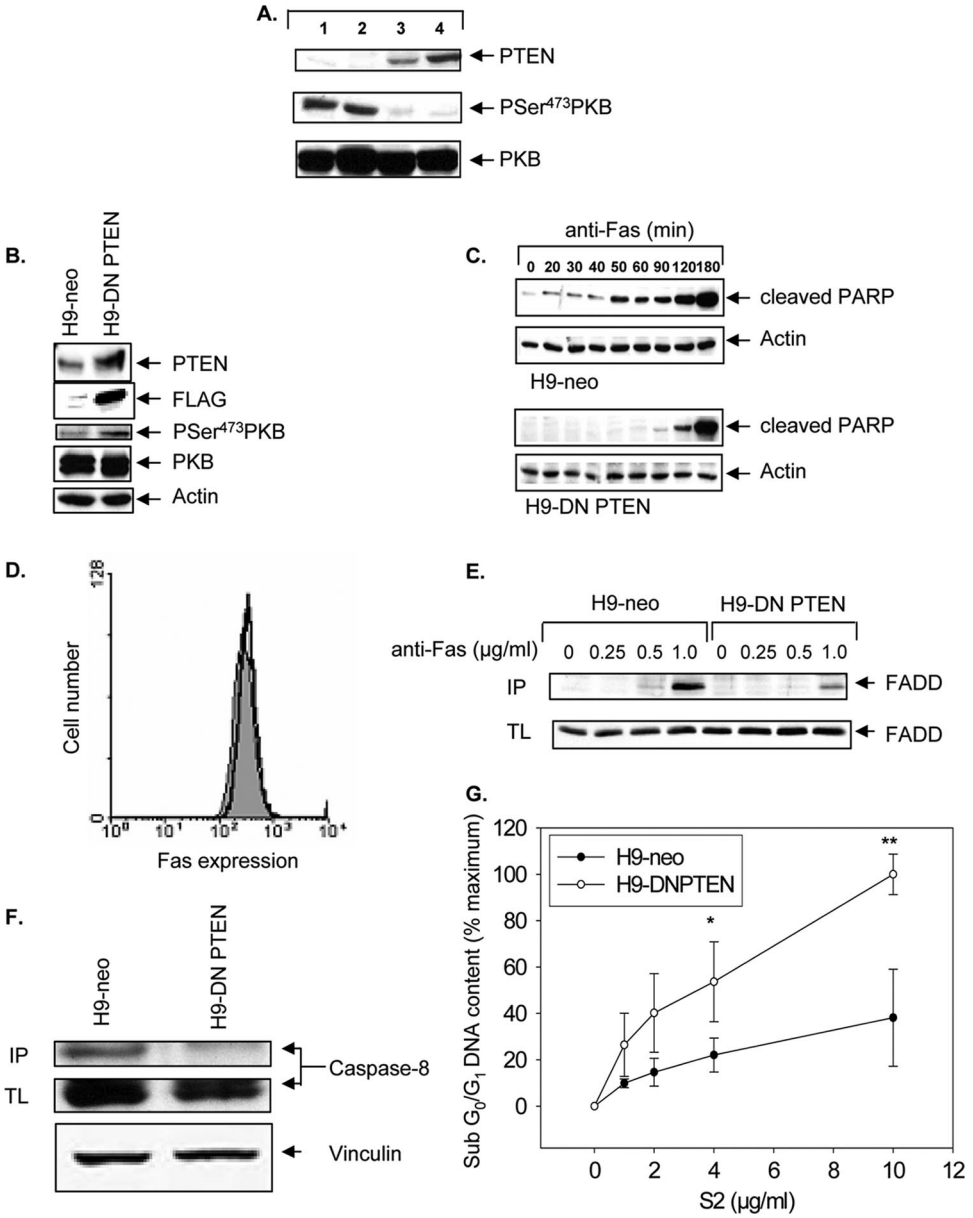

FIG. 1. Loss of PTEN and constitutive PKB activity correlate with the type II Fas phenotype, and stable expression of DN PTEN in type I cells induces delayed type II-like kinetics of PARP cleavage and acquisition of enhanced sensitivity to soluble FasL (S2), a selective cytotoxic agent for type II cells. (A) Immunoblot analysis of phospho-serine 473-PKB and PTEN in type II Jurkat (lane 1) and CEM (lane 2) cells and type I H9 (lane 3) and SKW6.4 (lane 4) cells. Total PKB is shown as a loading control. (B) Characterization of DN PTEN-expressing type I H9 cells. Levels of DN PTEN were detected by immunoblotting for PTEN in whole-cell lysates or anti-FLAG immunoprecipitates. H9-DN PTEN clones exhibited increased PKB activation, as monitored by immunoblotting with anti-phospho-PKB Ser473. Total PKB and actin were used as loading controls. (C) Time course of Fas-induced apoptosis of H9-neo and H9-DN PTEN cells, monitored by immunoblot analyses of cleaved PARP. Actin was used as a loading control. Blots represent the same exposure performed on a single film. Data presented are representative of three independent clones of H9-DN PTEN cells. (D) Flow cytometric analysis of cell surface Fas in H9-neo (filled histogram) and H9-DN PTEN cells (overlaid black line). (E) Reduced recruitment of FADD to activated CD95 in H9-DN PTEN cells relative to that in H9-neo cells. CD95 was immunoprecipitated (IP) from either unstimulated cells (0) or cells stimulated with anti-Fas at the indicated concentrations. Expression of FADD in total cell lysates (TL) was similar in all treatments. Cellular lysates equivalent to 10^7 cells and immunoprecipitates were subjected to 12% sodium dodecyl sulfate-polyacrylamide gel electrophoresis and immunoblotted using anti-FADD monoclonal antibody. (F) Reduced caspase-8 protein in complex with the DISC in H9-DN PTEN cells. In parallel, cells were stimulated with APO-1 (1.0 μg/ml) and immunoprecipitated as described above (IP). Cellular lysates equivalent to 10^7 cells (TL) were immunoblotted with anti-caspase-8. The blot was reprobed with anti-vinculin as a loading control. (G) Apoptosis assay of H9-neo and H9-DN PTEN cells treated for 16 h with increasing doses of S2. Data represent flow cytometric quantification of sub-G_0/G_1 DNA content, presented as the mean and standard error of the mean (SEM) percentage of maximum apoptosis, carried out by staining with propidium iodide. The data are representative of three independent experiments. *, $P < 0.05$; **, $P < 0.005$.

TABLE 1. Low levels of PTEN protein are associated with type II phenotype[a]

Phenotype	RCI			*P* value[d]
	PTEN high	PTEN low	Total	
Type I[b]	9	3	12	0.017
Type II[c]	1	11	12	0.013
Total	10	14		
P value[d]	0.010	0.022		

[a] Type I and type II cells within the NCI-60 chemosensitivity panel of cell lines (1) were studied, and their respective PTEN protein expression levels, presented as relative chemiluminescence intensity (RCI) units as determined by S. Barnett, Merck (http://dtp.nci.nih.gov/mtweb), are shown. A threshold was set at 0.4125 RCI to achieve maximal separation between the type I and type II groups.

[b] The RCI for type I cell lines were as follows: SF-295, 0.0022; IGROV1, 0.067; LOX IMVI, 0.17; TK-10, 0.48; UO-31, 0.5; HOP-92, 0.56; CAKI-1, 0.62; ACHN, 0.745; A498, 0.86; and T-47D, 0.885. The prototypic lymphoid cell lines H9 and SKW6.4 were included as PTEN wild-type type I cells.

[c] The RCI for type II cell lines were as follows: KM12, 0; UACC-62, 0.0362; CCRF-CEM, 0.11; NCI-H322 M, 0.19; BT-549, 0.19; NCI-H226, 0.23; HCT-116, 0.25; HCT-15, 0.28; NCI-H460, 0.285; RPMI-8226, 0.345; and SR, 1.34. The Jurkat cell line was included as type II and PTEN deficient, as shown in Fig. 1.

[d] *P* values were calculated using binomial distribution statistics.

PARP cleavage similar to that seen in type II Jurkat and CEM cells (34).

The prototype type I H9 cells exhibit strong Fas-induced DISC formation characterized by an abundance of FADD and caspase-8 recruited to the DISC, whereas prototype type II cells, such as Jurkat cells, form a weaker DISC associated with reduced recruitment of FADD and caspase-8 (34). We next tested whether DN PTEN could impair Fas DISC formation in type I H9 cells. Our analysis showed weaker DISC formation in H9-DN PTEN cells, as demonstrated by reductions in the amounts of FADD (Fig. 1E) and caspase-8 (Fig. 1F) recruited to the DISC compared to those in H9-neo cells, consistent with a type I-to-type II transition.

The soluble Fas ligand S2 is a more potent inducer of apoptosis in type II than in type I cells (1). We thus tested whether H9-DN PTEN cells would acquire enhanced S2 sensitivity, providing further support for a type I-to-type II phenotypic transition. Indeed, despite having reduced sensitivity to the multimeric FasL LzFasL (data not shown), H9-DN PTEN cells were more sensitive to S2 cytotoxicity, in a dose-dependent manner, than H9-neo cells (Fig. 1G). Collectively, these data indicate that PTEN inactivation can promote a transition from a type I to a type II-like Fas apoptosis signaling pathway.

Reexpression of PTEN or blockade of PI3K promotes type I-like signaling kinetics in type II cells. To assess whether blockade of PI3K in type II cells could induce type II cells to undergo a transition to a type I-like phenotype, PTEN-deficient type II Jurkat-T and CEM cells were stimulated with anti-Fas antibody for the indicated times in the presence of LY294002, a potent inhibitor of PI3K (44) (Fig. 2). Upon anti-Fas stimulation, LY294002 treatment of type II Jurkat-T cells resulted in acceleration of PARP cleavage compared to that in untreated Jurkat-T cells, which displayed predicted type II kinetics as previously reported (Fig. 2A and B) (34). Similar results were obtained in parallel anti-Fas time course experiments with type II CEM cells (data not shown). No PARP cleavage was observed in cells treated with LY294002 alone throughout the entire time course (data not shown). The kinetics of caspase-3 activation upon reintroduction of PTEN to Jurkat-T cells was examined in response to anti-Fas stimulation by flow cytometric analysis of intracellular active caspase-3 as previously described (3). Reintroduction of PTEN into Jurkat-T cells significantly accelerated the kinetics of caspase-3 activation (Fig. 2C). These data demonstrate that type I-like kinetics of Fas-induced signals can be restored in type II PTEN null cells by PI3K inhibition or PTEN expression.

PTEN expression or PI3K blockade unmasks mitochondrially independent type I-like Fas-induced apoptosis pathway in type II cells. The true acid test to discriminate between type I and type II cells is the ability of Bcl-2 overexpression to suppress Fas-mediated apoptosis in type II but not in type I cells (34). To determine whether the PTEN/PI3K pathway regulates the mitochondrial dependence of Fas-induced apoptosis in type I and type II cells, we examined whether treatment with LY294002 could alter the ability of Bcl-2 expression to protect

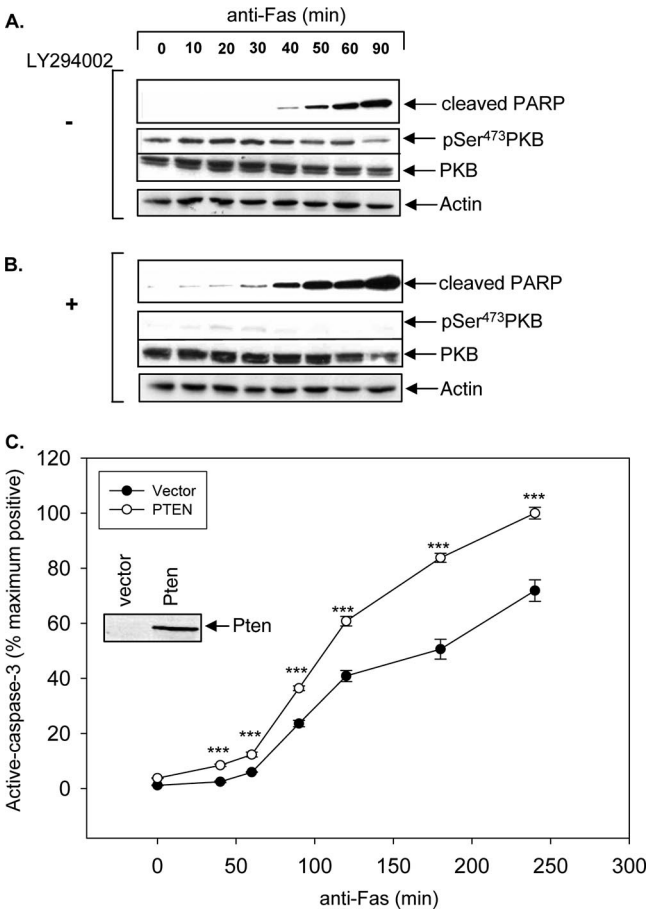

FIG. 2. Reexpression of PTEN or inhibition of PI3K with LY294002 induces type II cells to undergo type I-like kinetics of caspase-3 activation. Jurkat cells were pretreated for 2 h with DMSO as a control (A) or with 10 μM LY294002 (B). Cells were stimulated with 250 ng/ml anti-Fas (CH11) antibody in 0.1% serum for the indicated times. Immunoblot analysis detecting cleaved PARP (a marker of caspase-3 activation), phospho-PKB (pSer473), and total PKB levels is shown. (C) Time course of anti-Fas-induced apoptosis of Jurkat-T cells transiently transfected with vector alone or wild-type PTEN. The data represent the mean and SEM percentages of the maximum number of positive cells expressing intracellular active caspase-3. The results shown are representative of anti-Fas stimulations performed in triplicate. ***, $P < 0.0005$.

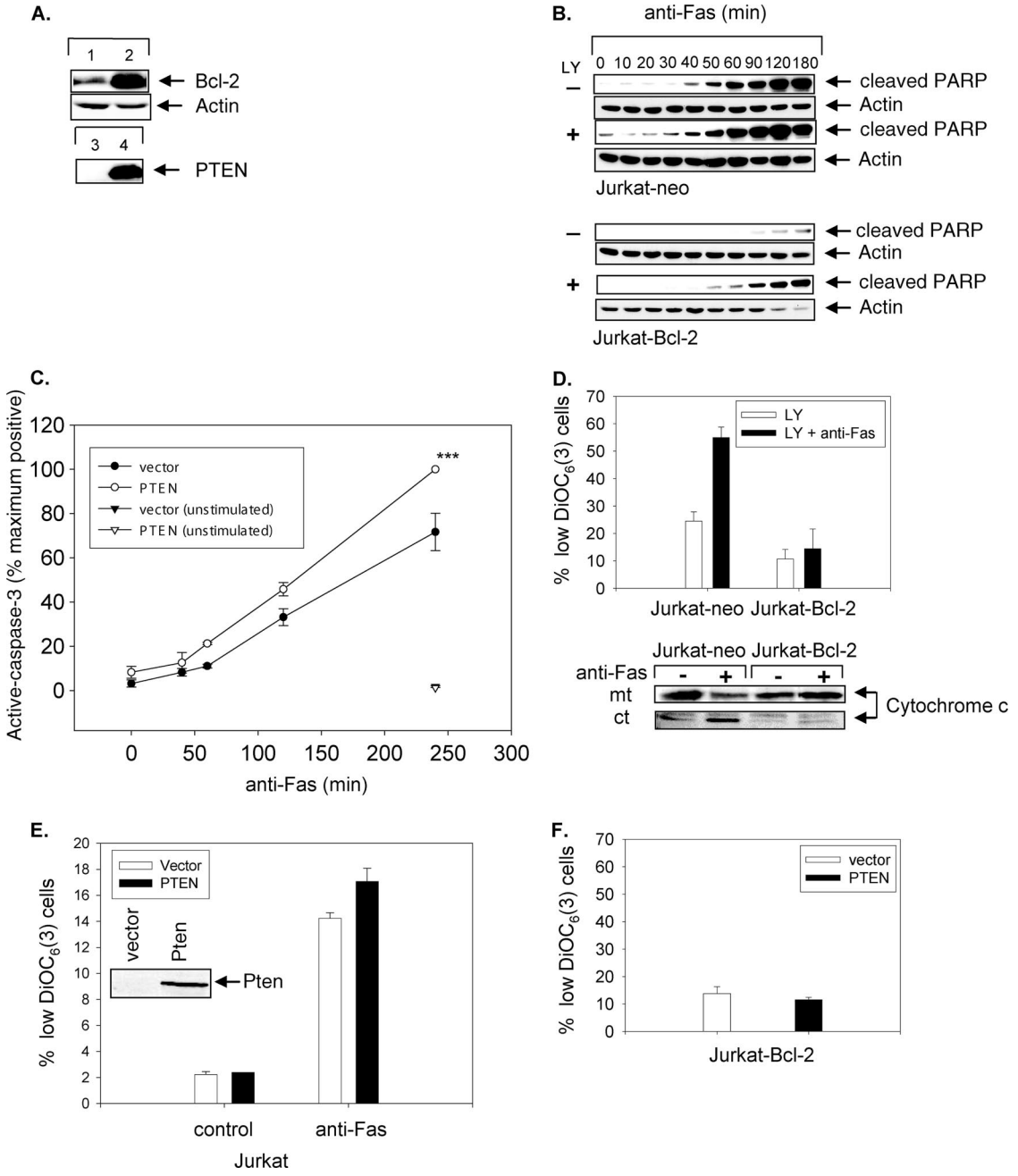

FIG. 3. PTEN expression or PI3K inhibition sensitizes PTEN-deficient type II Jurkat cells to mitochondrially independent Fas-induced apoptosis. (A) Bcl-2 protein expression in Jurkat-neo (lane 1) and Jurkat-Bcl-2 (lane 2) cells. PTEN protein expression in Jurkat-Bcl-2 vector-transfected cells (lane 3) and PTEN-transfected Jurkat-Bcl-2 cells (lane 4) is also shown. (B) Time course of Fas-induced apoptosis in Jurkat-neo (upper panels) or Jurkat-Bcl-2 (lower panels) cells pretreated with 10 μM LY294002 (+) or DMSO (−) for 2 h. A Western blot of cleaved PARP is shown. (C) Percentage of cells expressing intracellular active caspase-3 in Jurkat-Bcl-2 cells transiently transfected with either vector alone or PTEN following stimulation with anti-Fas for various lengths of time, as indicated, or after being left unstimulated for 4 h. Data represent the means and SEM for cells expressing active caspase-3, presented as the percentages of maximum achievable apoptosis in experiments performed in triplicate. ***, $P < 0.0005$. (D) Changes in $\Delta\Psi_m$ and levels of mitochondrial (mt) and cytoplasmic (ct) cytochrome *c* from Jurkat-neo and Jurkat-Bcl-2 cells pretreated with LY294002 (10 μM) prior to stimulation in the absence or presence of anti-Fas (CH11) antibody (250 ng/ml) for 90 min. (E) Effect of transient expression of PTEN on $\Delta\Psi_m$ of Jurkat cells. A PTEN immunoblot is shown (inset). (F) Absence of $\Delta\Psi_m$ in Jurkat-Bcl-2 cells transiently transfected with vector or PTEN followed by treatment with anti-Fas (CH11) for 4 h. Cells were analyzed by flow cytometry for $\Delta\Psi_m$, using the fluorochrome $DiOC_6$ (3). The mean (%) and SEM for cells with low $\Delta\Psi_m$ are shown. Experiments were performed in triplicate.

type II Jurkat cells from Fas-induced apoptosis. To this end, we treated Jurkat-neo (control vector-transfected Jurkat cells) (Fig. 3A, lane 1) or Jurkat-Bcl-2 (Bcl-2-overexpressing Jurkat cells) (Fig. 3A, lane 2) cells in the presence or absence of LY294002 and then stimulated the cells with anti-Fas in a time course study (Fig. 3B). As predicted, in the absence of LY294002 treatment caspase activation measured by PARP cleavage was impaired in Jurkat-Bcl-2 cells (Fig. 3B) (34). In

contrast, type I-like kinetics of PARP cleavage were observed in LY294002-treated Jurkat-Bcl-2 cells, demonstrating that LY294002 treatment promoted Bcl-2 insensitivity of Fas-induced apoptosis (Fig. 3B). In fact, the kinetics of PARP cleavage in LY294002-treated Jurkat-Bcl-2 cells was remarkably similar to the kinetics observed in the untreated Jurkat-neo cells. Thus, PI3K inhibition promotes Bcl-2-independent Fas-induced apoptosis of type II Jurkat cells.

We next assessed whether reinitiation of the mitochondrially independent Fas apoptosis pathway could also be achieved by reintroduction of PTEN into type II cells. PTEN expression in Jurkat-Bcl-2 cells resulted in accelerated kinetics of caspase-3 activation following Fas stimulation in PTEN-transfected Jurkat-Bcl-2 cells (Fig. 3C). There was no detectable increase over basal active caspase-3 levels in PTEN-expressing Jurkat-Bcl-2 cells compared to the vector control over the entire course of the experiment (Fig. 3C). As an additional experimental control to confirm that Bcl-2 expression could maintain protection of mitochondrial integrity despite LY294002 treatment or PTEN expression, we analyzed the ability of Bcl-2 to inhibit changes in $\Delta\Psi_m$ following Fas stimulation, using $DiOC_6(3)$ flow cytometric analysis of cells treated with LY294002 or expressing PTEN. As expected, Bcl-2 expression equally inhibited Fas-induced $\Delta\Psi_m$ and the release of cytochrome *c* from isolated mitochondria in either the presence or absence of LY294002 (Fig. 3D and data not shown). Furthermore, transient PTEN expression did not alter the Fas-induced collapse of mitochondrial potential in Jurkat (Fig. 3E) and Jurkat-Bcl-2 cells (Fig. 3F). Therefore, LY294002 treatment or PTEN expression does not affect the ability of Bcl-2 to protect the integrity of the mitochondria. Taken together, these results suggest that blockade of PI3K or reintroduction of PTEN into type II cells promotes the conversion to mitochondrially independent, Bcl-2-independent Fas-induced apoptosis.

PTEN heterozygosity confers sensitivity to Bcl-2 cytoprotection by thymocytes and T cells undergoing Fas-induced apoptosis and AICD, respectively. Transgenic *Bcl-2* expression is unable to suppress Fas-induced cell death of primary thymocytes and activated peripheral T lymphocytes, and thus these cells have previously been classified as mitochondrially independent type I cells (37, 47). *Pten*$^{+/-}$ mice display impaired Fas sensitivity and develop a lymphoproliferative disorder reminiscent of that in Fas- and FasL-deficient mice (11). To test whether impaired Fas-induced apoptosis observed in *Pten*$^{+/-}$ mice could be due to a transition from mitochondrially independent type I to mitochondrially dependent type II Fas signaling, we investigated whether transgenic *Bcl-2* expression could protect *Pten*$^{+/-}$ thymocytes from Fas-mediated cell death. The relative sensitivities of thymocytes derived from wild-type, *Pten*$^{+/-}$ (29), Eμ-bcl-2-36 transgenic (*Eμ-bcl-2*; Jackson Laboratories, Bar Harbor, ME), and *Pten*$^{+/-}$; *Eμ-bcl-2* mice to Fas-induced apoptosis were determined by a subdiploid DNA flow cytometric assay. Bcl-2 overexpression may protect thymocytes in the absence of any Fas treatment, but not against Fas-dependent apoptosis. *Pten*$^{+/-}$; *Eμ-bcl-2* thymocytes exhibited reduced sensitivity to Fas-mediated cell death, in a dose-dependent manner (Fig. 4A), compared to that of *Pten*$^{+/-}$ thymocytes. In addition, the rate of Fas-mediated death was also diminished for *Pten*$^{+/-}$; *Eμ-bcl-2* thymocytes compared with that for *Pten*$^{+/-}$ thymocytes in a time course experiment (data not shown).

Reactivation of T lymphoblasts via receptor cross-linking triggers AICD in a Fas/FasL-dependent manner (17). In addition, analyses of *bcl-2* transgenic mice demonstrated that AICD of T cells is mitochondrially independent (37), indicating that AICD is mediated by a type I Fas response. To determine whether Pten haploinsufficiency induces a switch in Fas-dependent AICD of T cells from a mitochondrially independent type I to a mitochondrially dependent type II response, we investigated whether transgenic *bcl-2* expression was capable of suppressing AICD of peripheral T lymphocytes from *Pten*$^{+/-}$ mice. Activated T cells from wild-type, *Eμ-bcl-2*, *Pten*$^{+/-}$, and *Pten*$^{+/-}$; *Eμ-bcl-2* mice were plated on anti-CD3 antibody-coated wells in the presence of IL-2. The relative apoptosis was measured 24 h later, and the results are shown in Fig. 4B. The levels of AICD were similar in wild-type, *Eμ-bcl-2*, and *Pten*$^{+/-}$ activated T cells, whereas AICD in activated T lymphocytes from *Pten*$^{+/-}$; *Eμ-bcl-2* mice was impaired at all doses tested (Fig. 4B). As expected, the addition of Fas-Fc chimeric protein blocked AICD, consistent with previous observations (6) that AICD is Fas dependent (data not shown). Taken together, these data demonstrate that Pten haploinsufficiency promotes a transition in Fas-induced cell death from a mitochondrially independent to a mitochondrially dependent apoptotic response in primary thymocytes and activated peripheral T cells.

Loss of PTEN enhances PEA-15 phosphorylation at serine 116 and binding to FADD, and overexpression of phosphomimetic S116D PEA-15 in type I H9 cells leads to type II-like kinetics of caspase-3 activation in response to Fas stimulation. In an attempt to determine how PTEN might control type I versus type II Fas signals, we analyzed the Affymetrix gene expression profiling data set generated from the NCI-60 chemosensitivity panel of tumor lines (36) to identify PTEN-regulated genes that are differentially expressed in type I versus type II cells. From data mining analyses of this 6,800-gene set, we identified a number of genes that were able to strongly discriminate between type I and type II cells and which were associated with PTEN expression status based on the Wilcoxon two-sample test (data not shown). Among the top five genes that best discriminate between type I and type II cells, we identified PEA-15/PED ($P = 1.17 \times 10^{-5}$) as the most likely PTEN-regulated gene candidate that may be capable of regulating type I versus type II Fas signaling. PEA-15 was originally identified as a ubiquitously expressed 15-kDa antiapoptotic protein containing a death effector domain (DED) that is able to regulate Fas-, Trail-, and tumor necrosis factor (TNF)-mediated apoptosis (7, 13). Phosphorylation of PEA-15 at serine 116 (Ser116) promotes its binding to FADD and suppresses Fas DISC formation. Importantly, PKB has been shown to phosphorylate PEA-15 at Ser116, and phosphorylation at this site contributes to the antiapoptotic activity of PEA-15 (43). Therefore, since PTEN and PI3K are key regulators of PKB activity, we investigated whether PTEN expression or PI3K inhibition could regulate the levels of phosphorylation of PEA-15 on Ser116 (phospho-[Ser116]-PEA-15). We first compared the phospho-[Ser116]-PEA-15 levels in type II PTEN null Jurkat cells versus type I PTEN-expressing H9 cells. Jurkat cells exhibited higher basal phospho-[Ser116]-PEA-15

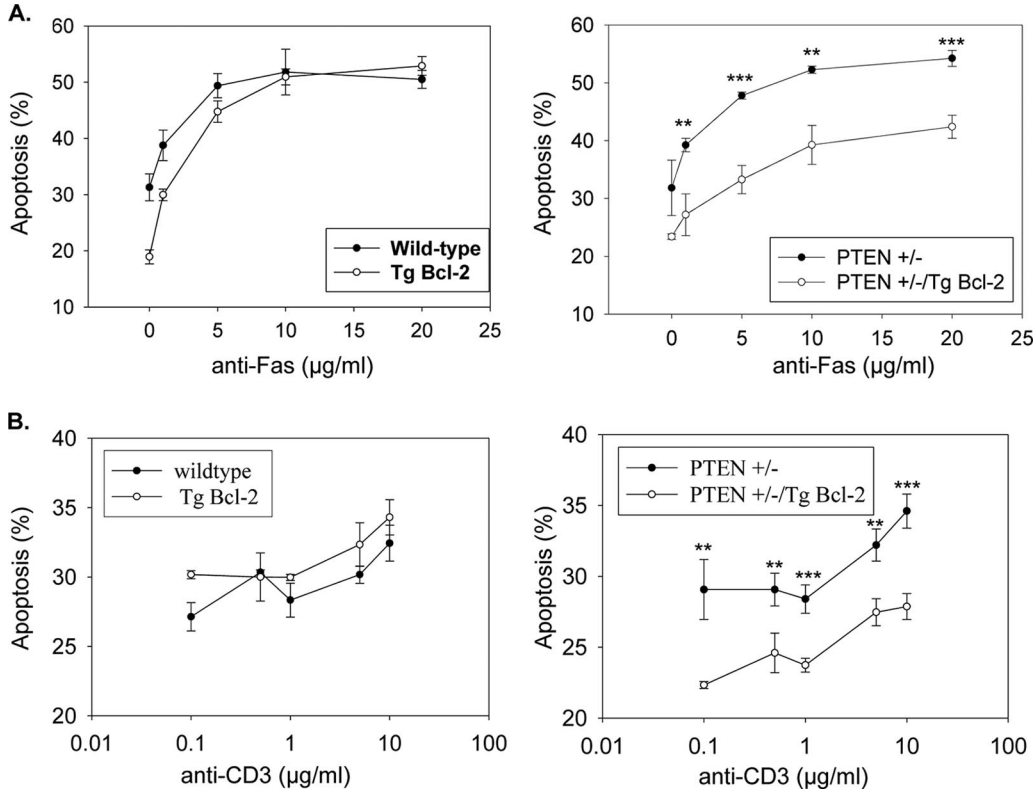

FIG. 4. PTEN haploinsufficiency converts Fas-induced apoptosis of type I primary thymocytes and activated T cells to a type II Bcl-2-sensitive response. (A) Dose-dependent Fas-mediated apoptosis of thymocytes isolated from wild-type and *Eμ-bcl-2* (Tg Bcl-2) mice (left panel) and from *Pten*$^{+/-}$ and *Pten*$^{+/-}$; *Eμ-bcl-2* mice (right panel). Data represent the mean and SEM amounts of subdiploid DNA accumulated after 24 h of anti-Fas stimulation performed in triplicate. (B) Reduced AICD in *Pten*$^{+/-}$; *Eμ-bcl-2* activated T cells (right panel). Viable activated T cells were seeded on plate-bound anti-CD3 in triplicate at the indicated concentration for 24 h. The data represent the mean and SEM percentages of cells undergoing apoptosis, as determined by subdiploid DNA content. Spontaneous apoptosis from controls was subtracted from the values for the corresponding treated samples. **, $P < 0.005$; ***, $P < 0.0005$.

levels than did H9 cells, while both Jurkat and H9 cells expressed similar levels of PEA-15 (Fig. 5A). Furthermore, LY294002 treatment of type II Jurkat cells also inhibited Ser116 phosphorylation of PEA-15 that was associated with decreased levels of phospho-PKB (Fig. 5B). Next, to test whether PTEN expression could regulate PEA-15 phosphorylation at Ser116, we examined phospho-[Ser116]-PEA-15 levels in Tet-on PTEN LNCaP cells that express PTEN in a doxycycline (Dox)-inducible manner (3). Tet-on PTEN LNCaP cells were treated in the presence or absence of Dox, and in parallel, PTEN-deficient LNCaP parental cells were treated with or without LY294002. Dox treatment of Tet-on PTEN LNCaP cells led to increased PTEN expression and a corresponding decrease in PKB phosphorylation (Ser473) (Fig. 5C). As expected, LY294002 treatment of parental LNCaP cells effectively blocked PKB phosphorylation at Ser473 (Fig. 5C). Both the reexpression of PTEN and the blockade of PI3K inhibited the levels of phospho-[Ser116]-PEA-15 (Fig. 5C), indicating that PTEN expression and PI3K inhibition can regulate the phosphorylation of PEA-15 at Ser116.

Next, we investigated whether expression of DN PTEN in type I H9 cells, which induces a conversion to a type II-like phenotype, is associated with concomitant increases in PEA-15 phosphorylation on Ser116 and in PEA-15 binding to FADD. Our analyses revealed that H9-DN PTEN cells exhibited increased levels of phospho-[Ser116]-PEA-15 compared to H9-vector cells (Fig. 5D). Furthermore, the expression of DN PTEN reduced DISC-associated FADD and phospho-[Ser116]-PEA-15, in association with a concomitant increase in FADD binding to PEA-15 (Fig. 5E). To assess the effect of PEA-15 phosphorylation on DISC formation and apoptosis, we introduced a phosphomimetic Asp mutation into PEA-15 at position Ser^{116} (PEA-15 S116D). The FLAG-tagged PEA-15 S116D protein was expressed in H9 cells, and the amount of FADD recruitment to the DISC upon Fas stimulation was assessed. Overexpression of PEA-15 S116D in H9 cells reduced FADD recruitment to the DISC compared to that in H9 cells expressing wild-type PEA-15 or empty vector controls (Fig. 5F). Consistent with this finding, the expression of PEA-15 S116D in H9 cells suppressed Fas-induced apoptosis, as monitored by flow cytometric detection of cleaved caspase-3 (Fig. 5G), which is consistent with a switch to a delayed type II-like kinetics of caspase-3 activation. Taken together, these data suggest that the loss of PTEN function may mediate a transition toward a type II-like phenotype by activating PI3K/PKB, which in turn induces phosphorylation of PEA-15 at Ser116, promoting its association with FADD

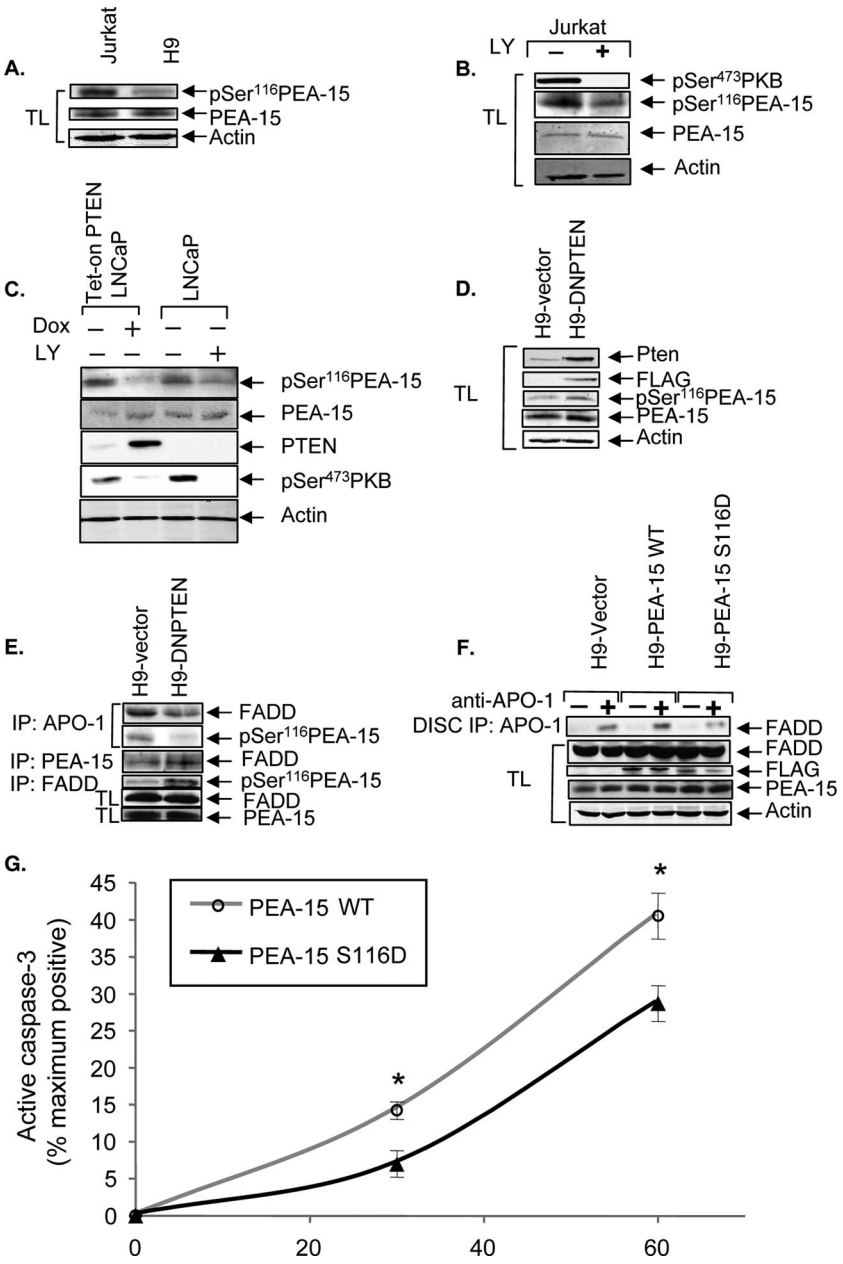

FIG. 5. PTEN regulates phosphorylation of PEA-15, and overexpression of a phosphomimetic mutant of PEA-15 in type I H9 cells causes them to undergo type II-like kinetics of caspase-3 activation. (A) PEA-15 expression and phosphorylation status in type II Jurkat and type I H9 cells. The levels of endogenous phospho-[Ser116]-PEA-15 and total PEA-15 in whole-cell lysates from cells serum starved for 4 h are shown. The blot was stripped and reprobed for actin as a loading control. (B) The effects of PI3K inhibition on the phosphorylation status of PKB and PEA-15 were monitored by immunoblotting for phospho-[Ser473]-PKB and phospho-[Ser116]-PEA-15 in whole-cell lysates (TL) of Jurkat cells treated with DMSO or LY294002 (40 μM) for 4 h. The blot was stripped and reprobed to demonstrate the level of total PEA-15. The same blot was probed with anti-actin as a loading control. (C) Tet-on PTEN LNCaP cells were treated with or without Dox (4 μg/ml) for 48 h in medium containing 10% serum. Serum was then withdrawn for an additional 48 h. Parental LNCaP cells were treated in parallel with either DMSO or LY294002 (40 μM) for 48 h in the absence of serum. The levels of PTEN, phospho-[Ser473]-PKB, phospho-[Ser116]-PEA-15, and total PEA-15 in whole-cell lysates are shown. Actin was used as a loading control. (D) DN PTEN expression in H9 cells. Lentivirus-driven DN PTEN expression was detected by immunoblotting with anti-PTEN and anti-FLAG antibodies. The levels of total PEA-15 and phospho-[Ser116]-PEA-15 in H9-DN PTEN cells compared to those in vector controls are shown. Actin was used as a loading control. (E) DISC-associated FADD in H9-vector and H9-DN PTEN cells. FADD-associated PEA-15 and total FADD in H9-DN PTEN cells are shown compared to those in H9-vector cells. Phospho-[Ser116]-PEA-15 associated with FADD and total PEA-15 levels in H9-vector and H9-DN PTEN cells are also shown. (F) DISC-associated FADD in H9-vector, H9-PEA-15 WT, and H9-PEA-15 S116D cells. The levels of exogenous PEA-15 WT and PEA-15 S116D were demonstrated by reprobing the blot with anti-FLAG. The levels of total PEA-15, FADD, and actin are shown to demonstrate equal loading of whole-cell lysates. (G) Time course (0 to 60 min) of apoptosis induced by anti-Fas (0.5 μg/ml), as measured by flow cytometric analyses of intracellular active caspase-3 in H9 cells stably expressing PEA-15 WT or PEA-15 S116D. Data represent the means and SEM for cells expressing active caspase-3, presented as percentages of the maximum achievable apoptosis in experiments performed in triplicate and corrected by subtracting the level of spontaneous apoptosis of untreated control cells. *, $P < 0.05$.

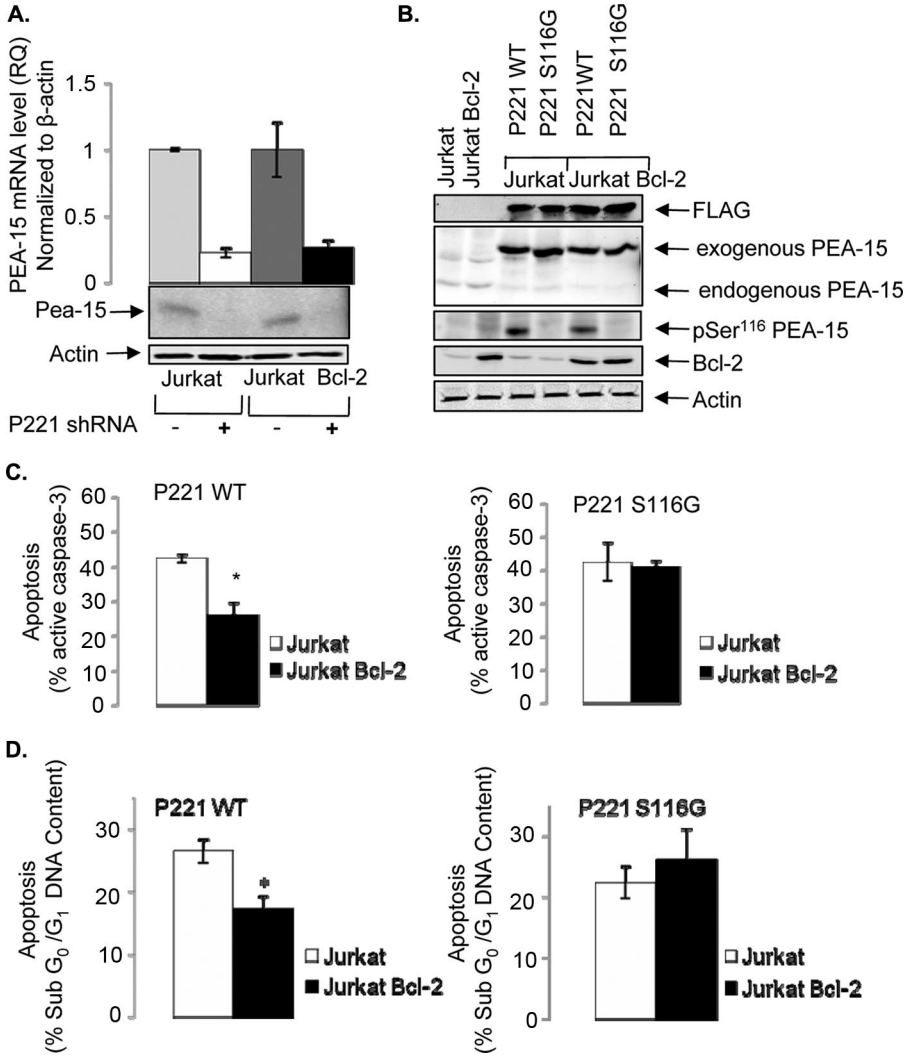

FIG. 6. Bcl-2 mediated protection of Fas apoptosis is dependent on PEA-15 Ser116 phosphorylation. (A) Relative quantities (RQ) of PEA-15 mRNA in Jurkat and Jurkat-Bcl-2 cells expressing P221 shRNA, as shown by qPCR and immunoblotting. Actin was used as an endogenous control for qPCR and as a loading control for the Western blot. RQ values were calculated from ΔC_T values for Jurkat (RQ = 1), Jurkat P221 (RQ = 0.223), Jurkat-Bcl-2 (RQ = 1), and Jurkat-Bcl-2 P221 (RQ = 0.263) cells. (B) Immunoblot analyses showing the expression of PEA-15 WT or PEA-15 S116G in reconstituted Jurkat P221 and Jurkat-Bcl-2 P221 cells. The exogenous expression and endogenous knockdown of total PEA-15 are also shown. The levels of phospho-[Ser116]-PEA-15 and Bcl-2 are shown. Actin was used to demonstrate equal loading of whole-cell lysates. (C). Percent (%) apoptosis, as measured by the level of active caspase-3 triggered by anti-Fas (250 ng/ml CH11) stimulation of Jurkat P221 and Jurkat-Bcl-2 P221 cells reconstituted with either PEA-15 WT or PEA-15 S116G for 4 h. (D) Fas-induced (50 ng/ml CH11) apoptosis, as monitored by the percentage of cells containing sub-G_0/G_1 DNA content after 20 h of treatment of Jurkat P221 and Jurkat-Bcl-2 P221 cells reconstituted with either PEA-15 WT or PEA-15 S116G. Bars are representative of the means and SEM for experiments performed twice in triplicate. In all cases, the level of spontaneous apoptosis was subtracted from the level of specific apoptosis determined by flow cytometry. *, $P < 0.01$.

and consequently suppressing DISC formation and Fas-induced apoptosis.

PEA-15 phosphorylation on Ser116 regulates Bcl-2 sensitivity of Fas-induced apoptosis of Jurkat cells. The most rigorous and definitive standard to discriminate between type I and type II cells is the ability of Bcl-2 expression to protect type II but not type I cells from Fas-induced apoptosis. To examine whether PEA-15 is able to regulate Bcl-2 sensitivity of Fas-induced apoptosis of type II Jurkat cells in a phosphorylation-dependent manner, we silenced endogenous PEA-15 expression in Jurkat and Jurkat-Bcl-2 cells by using a PEA-15-specific shRNA targeting codons 221 or 250 (P221 shRNA) and reconstituted the cells with a vector expressing either wild-type or nonphosphorylatable S116G mutant PEA-15 that is refractory to shRNA silencing by containing multiple silent third-codon point mutations within the shRNA target region. As shown in Fig. 6A, the expression of P221 shRNA in Jurkat and Jurkat-Bcl-2 cells resulted in >70% silencing of PEA-15 expression. Next, we reconstituted Jurkat P221 and Jurkat-Bcl-2 P221 cells with P221 shRNA-refractory cDNA encoding a FLAG-tagged nonphosphorylatable PEA-15 mutant (PEA-15 S116G) or a PEA-15 wild-type rescue (PEA-15 WT-rescue) and compared their sensitivities to Fas-induced apoptosis. By immunoblotting with anti-FLAG and anti-PEA-15 antibodies, we observed sim-

ilar expression levels of PEA-15 WT-rescue and PEA-15 S116G in both Jurkat P221 and Jurkat-Bcl-2 P221 cells (Fig. 6B). In addition, we observed minimal PEA-15 Ser116 phosphorylation in Jurkat P221 or Jurkat-Bcl-2 P221 cells that expressed the PEA-15 S116G rescue cDNA (Fig. 6B). Next, cells were treated with anti-Fas (CH11; 250 ng/ml) for 4 h, and the level of active caspase-3 induction was measured by flow cytometry. As expected, the level of cleaved caspase-3 production in Jurkat-Bcl-2 P221 WT-rescue cells was significantly inhibited compared to that in Jurkat P221 WT-rescue cells ($P < 0.01$), consistent with the ability of Bcl-2 to protect type II Jurkat cells from Fas-induced apoptosis. Importantly, there was no significant difference in cleaved caspase-3 in Jurkat P221 and Jurkat-Bcl-2 P221 cells that expressed the phosphorylation-defective PEA-15 S116G mutant compared to that in Jurkat P221 WT-rescue cells (Fig. 6C), indicating that Bcl-2 could not protect Jurkat cells expressing a nonphosphorylatable PEA-15 mutant from Fas-induced apoptosis. Consistently, when we treated the cells with anti-Fas (CH11; 50 ng/ml) and measured the percentage of cells undergoing DNA fragmentation after 20 h of treatment, apoptosis induction measured by sub-G_0/G_1 DNA content was significantly inhibited in Jurkat-Bcl-2 P221 PEA-15 WT-rescue cells compared to that in Jurkat P221 PEA-15 WT-rescue cells but not in Jurkat P221 PEA-15 S116G and Jurkat-Bcl-2 P221 PEA-15 S116G cells, which maintained similar sensitivities to Fas (Fig. 6D). Taken together, these data indicate that PEA-15 Ser116 phosphorylation is important for mediating the Bcl-2 sensitivity of type II Jurkat cells in response to Fas stimulation and that the mitochondrial dependence of type II cells is regulated by PTEN via PEA-15.

DISCUSSION

In this study, we demonstrate that Fas-induced apoptotic signaling in type I and type II cells is determined, at least in part, by integrative signals delivered by the PTEN/PI3K pathway. Previous reports have implicated the PTEN/PI3K pathway in regulating Fas-induced apoptosis (11, 18, 21, 39, 48); however, its role in regulating type I versus type II Fas signals is unknown. Here we show, through gain-of-function and loss-of-function approaches, that PTEN inactivation is able to delay the kinetics of caspase activation, suppress DISC formation, and promote increased dependence of Fas signaling on the intrinsic mitochondrial apoptotic pathway in mediating apoptosis, which collectively is consistent with a transition to a type II phenotype. Furthermore, we now show that PTEN inactivation leads to increased levels of phospho-[Ser116]-PEA-15 that correspond with a concomitant increase in binding of PEA-15 to FADD and decrease in DISC recruitment of FADD, suggesting that PTEN inactivation promotes PEA-15 binding to FADD and suppresses DISC formation by sequestering FADD from the Fas DISC. Furthermore, Bcl-2 was able to suppress Fas-induced apoptosis in Jurkat cells reconstituted with wild-type PEA-15 but not with a nonphosphorylatable S116G mutant of PEA-15. Collectively, these data suggest that Fas-induced apoptosis in type I and type II cells is determined, at least in part, by the PTEN/PI3K signaling pathway through regulation of the phosphorylation and activity of PEA-15.

PEA-15 is a 15-kDa phosphoprotein that contains a DED (30). PEA-15 has been shown to bind to FADD and caspase-8 via homotypic DED interactions, which displaces the association of FADD and caspase-8 and suppresses DISC formation (7, 22). Phosphorylation of PEA-15 at Ser116 is required to promote FADD binding (31), and PEA-15 is known to be phosphorylated at Ser116 by both PKB and CaMKII (23, 43). We have found that the loss of PTEN promotes increased phosphorylation of PEA-15 at Ser116 and leads to increased association of PEA-15 with FADD and decreased levels of FADD at the Fas DISC. PTEN inactivation promotes constitutive activation of PKB (26). Furthermore, PKB has been shown to bind to and phosphorylate PEA-15 at Ser 116 (43). Therefore, we propose a model (Fig. 7) wherein PTEN plays a key role in determining the differential Fas death receptor signals in type I and type II cells via regulating the phosphorylation of PEA-15 at Ser 116. Loss of PTEN leads to PKB activation and PKB-mediated phosphorylation of PEA-15 at Ser116, which in turn allows PEA-15 to bind to and suppress DISC formation by sequestering FADD from the Fas DISC, leading to weak caspase-8 activation and increasing the dependence of Fas signaling on the mitochondrial apoptotic pathway, which are key classical features of Fas-induced apoptosis in type II cells. Concomitantly, phosphorylation of PEA-15 at Ser116 also leads to dissociation of PEA-15 from extracellular signal-regulated kinase (ERK), relieving the cytoplasmic sequestration of ERK and allowing ERK to translocate to the nucleus, where it mediates mitogenic functions. Furthermore, ERK has also been shown to prevent Fas-mediated apoptosis (12, 19, 20). ERK signaling is thought to attenuate the mitochondrial pathway of Fas-induced apoptosis, for example, via regulating p90rsk1-mediated phosphorylation and inactivation of the proapoptotic protein Bad (4, 41) and/or by directly phosphorylating and stabilizing Bcl-2 (5). Thus, the transition to the mitochondrially dependent type II apoptotic pathway may be mediated through the coordinated actions of PEA-15 association with FADD and inhibition of DISC formation as well as through ERK-mediated suppression and sensitization of the mitochondrial arm of Fas signaling.

Pten haploinsufficiency in mice leads to the development of a lymphoproliferative disorder reminiscent of that seen in Fas- and FasL-deficient mice (11). The precise mechanism by which Pten haploinsufficiency leads to impaired Fas apoptosis in vivo is unclear. We propose a model wherein reduction of PTEN leads to a type II Fas signaling pathway characterized by an increased dependence of the cells on the mitochondrial arm of the apoptotic pathway. This mitochondrially dependent type II pathway can then readily be protected through regulation of the tone of the intrinsic apoptotic response in vivo by integrated signals derived from chemokines, growth/survival factors, adhesion molecules, and/or costimulatory receptors from the host microenvironment, as originally postulated by Roy and Nicholson (32). For example, type II cells may readily become refractory to Fas-induced apoptosis in vivo as a result of upregulation of antiapoptotic proteins that block the intrinsic apoptotic pathway, such as Bcl-2, Bcl-xL, or IAPs induced by extracellular signals.

Downregulation of PTEN expression may be a normal physiological mechanism by which cells regulate type I/type II Fas sensitivity. Interestingly, long-term activated T cells that exhibit reduced sensitivity to Fas and impaired DISC formation

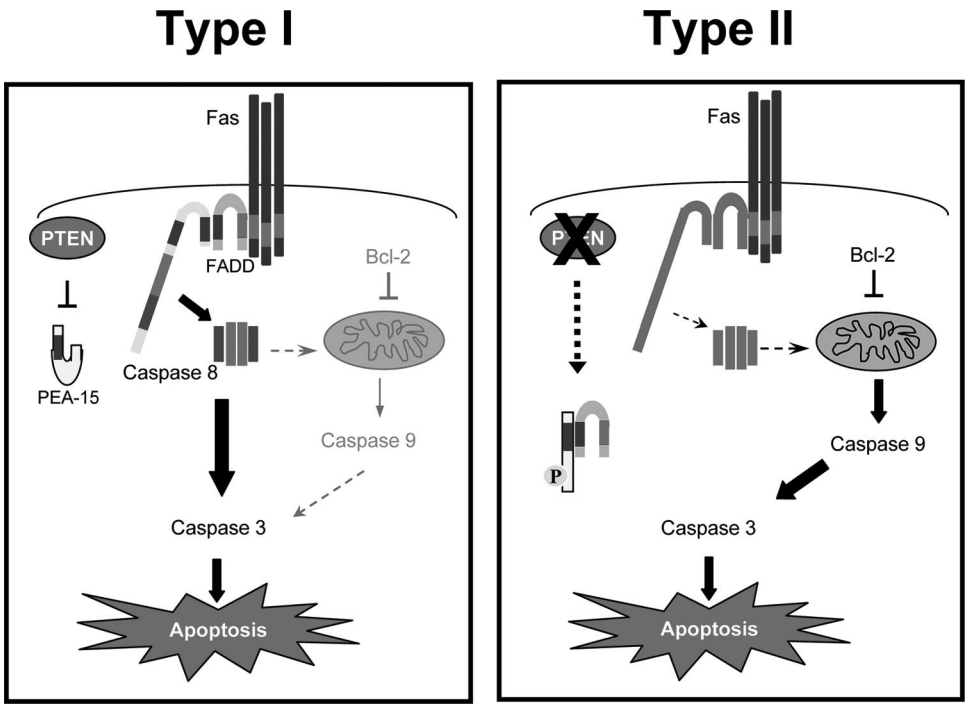

FIG. 7. Model of regulation of Fas type I versus type II signaling by PTEN via PEA-15. We propose a model wherein loss of PTEN converts cells to undergo mitochondrially dependent type II apoptosis in response to Fas via PEA-15. PTEN inactivation promotes increased phosphorylation of PEA-15 at Ser 116 that leads to attenuation of DISC formation via the binding of phospho-PEA-15 to FADD and sequestration of FADD from the Fas DISC.

display markedly reduced PTEN levels and elevated levels of phosphorylated PKB (38). Alternatively, cells may acquire a switch to type II Fas signaling through activation of PI3K signaling via growth factor/cytokine stimulation. For example, T-cell costimulation via CD28 has been shown to delay the kinetics of caspase activation, impair Fas-induced cell death, and reduce DISC formation in a PKB-dependent manner (21). Furthermore, hepatocyte growth factor stimulation of hepatomas has been shown to reduce Fas sensitivity and suppresses Fas DISC formation (40). Our data suggest that downmodulation of PTEN or growth factor/cytokine stimulation may lead to impaired DISC formation and reduced Fas sensitivity, in part through regulation of PEA-15 phosphorylation at Ser116.

Our studies show that PTEN status strongly correlates with the type I/type II phenotype of a wide array of tumor cell lines, such that 92% of type II cells are low PTEN expressers and 75% of type I cells are high PTEN expressers. This suggests that PTEN is a key player in determining whether a cell dies by a mitochondrially independent type I or mitochondrially dependent type II Fas-induced apoptotic mechanism. Additional signaling pathways may also integrate with the PTEN/PI3K/PEA-15 pathway in determining the routing of Fas apoptotic signals. For example, galectin-3 was recently implicated in regulating Fas-induced apoptosis of type I and type II cells (15). Consistent with our findings, the ability of galectin-3 expression to induce an accelerated type I-like kinetics of caspase activation in type II cells may be mediated, in part, by its ability to inhibit the activity of PKB, a key mediator of the PI3K/PTEN signaling pathway (24).

In summary, loss of the PTEN tumor suppressor promotes type II mitochondrially dependent Fas-induced apoptosis through its regulation of phosphorylation of PEA-15 on Ser116, which leads to the suppression of FADD recruitment to the DISC. Thus, our data collectively suggest that the PTEN/PI3K pathway may, in part, determine whether a cell dies by mitochondrially independent type I or mitochondrially dependent type II Fas-induced apoptosis via regulation of PEA-15 phosphorylation and binding to FADD.

ACKNOWLEDGMENTS

We thank Gerald Krystal for a critical review of the manuscript and Megan Levings for providing pLSXNΔNGFR.

This work was funded by the Canadian Institutes of Health Research. M.E.P. is supported by RO1 GM61712.

We have no conflicting financial interests.

REFERENCES

1. **Algeciras-Schimnich, A., E. M. Pietras, B. C. Barnhart, P. Legembre, S. Vijayan, S. L. Holbeck, and M. E. Peter.** 2003. Two CD95 tumor classes with different sensitivities to antitumor drugs. Proc. Natl. Acad. Sci. USA **100:** 11445–11450.
2. **Barnhart, B. C., E. C. Alappat, and M. E. Peter.** 2003. The CD95 type I/type II model. Semin. Immunol. **15:**185–193.
3. **Bertram, J., J. W. Peacock, C. Tan, A. L. Mui, S. W. Chung, M. E. Gleave, S. Dedhar, M. E. Cox, and C. J. Ong.** 2006. Inhibition of the phosphatidylinositol 3′-kinase pathway promotes autocrine Fas-induced death of phosphatase and tensin homologue-deficient prostate cancer cells. Cancer Res. **66:**4781–4788.
4. **Bonni, A., A. Brunet, A. E. West, S. R. Datta, M. A. Takasu, and M. E. Greenberg.** 1999. Cell survival promoted by the Ras-MAPK signaling pathway by transcription-dependent and -independent mechanisms. Science **286:** 1358–1362.
5. **Breitschopf, K., J. Haendeler, P. Malchow, A. M. Zeiher, and S. Dimmeler.** 2000. Posttranslational modification of Bcl-2 facilitates its proteasome-dependent degradation: molecular characterization of the involved signaling pathway. Mol. Cell. Biol. **20:**1886–1896.

6. **Brunner, T., R. J. Mogil, D. LaFace, N. J. Yoo, A. Mahboubi, F. Echeverri, S. J. Martin, W. R. Force, D. H. Lynch, C. F. Ware, et al.** 1995. Cell-autonomous Fas (CD95)/Fas-ligand interaction mediates activation-induced apoptosis in T-cell hybridomas. Nature **373:**441–444.
7. **Condorelli, G., G. Vigliotta, A. Cafieri, A. Trencia, P. Andalo, F. Oriente, C. Miele, M. Caruso, P. Formisano, and F. Beguinot.** 1999. PED/PEA-15: an anti-apoptotic molecule that regulates FAS/TNFR1-induced apoptosis. Oncogene **18:**4409–4415.
8. **Curtin, J. F., and T. G. Cotter.** 2003. Live and let die: regulatory mechanisms in Fas-mediated apoptosis. Cell. Signal. **15:**983–992.
9. **Desagher, S., A. Osen-Sand, S. Montessuit, E. Magnenat, F. Vilbois, A. Hochmann, L. Journot, B. Antonsson, and J. C. Martinou.** 2001. Phosphorylation of bid by casein kinases I and II regulates its cleavage by caspase 8. Mol. Cell **8:**601–611.
10. **Deveraux, Q. L., N. Roy, H. R. Stennicke, T. Van Arsdale, Q. Zhou, S. M. Srinivasula, E. S. Alnemri, G. S. Salvesen, and J. C. Reed.** 1998. IAPs block apoptotic events induced by caspase-8 and cytochrome c by direct inhibition of distinct caspases. EMBO J. **17:**2215–2223.
11. **Di Cristofano, A., P. Kotsi, Y. F. Peng, C. Cordon-Cardo, K. B. Elkon, and P. P. Pandolfi.** 1999. Impaired Fas response and autoimmunity in Pten+/− mice. Science **285:**2122–2125.
12. **Engedal, N., and H. K. Blomhoff.** 2003. Combined action of ERK and NF kappa B mediates the protective effect of phorbol ester on Fas-induced apoptosis in Jurkat cells. J. Biol. Chem. **278:**10934–10941.
13. **Estelles, A., C. A. Charlton, and H. M. Blau.** 1999. The phosphoprotein protein PEA-15 inhibits Fas- but increases TNF-R1-mediated caspase-8 activity and apoptosis. Dev. Biol. **216:**16–28.
14. **Fujita, E., Y. Kouroku, Y. Miho, T. Tsukahara, S. Ishiura, and T. Momoi.** 1998. Wortmannin enhances activation of CPP32 (caspase-3) induced by TNF or anti-Fas. Cell Death Differ. **5:**289–297.
15. **Fukumori, T., Y. Takenaka, N. Oka, T. Yoshii, V. Hogan, H. Inohara, H. O. Kanayama, H. R. Kim, and A. Raz.** 2004. Endogenous galectin-3 determines the routing of CD95 apoptotic signaling pathways. Cancer Res. **64:**3376–3379.
16. **Gibson, S., S. Tu, R. Oyer, S. M. Anderson, and G. L. Johnson.** 1999. Epidermal growth factor protects epithelial cells against Fas-induced apoptosis. Requirement for Akt activation. J. Biol. Chem. **274:**17612–17618.
17. **Green, D. R., N. Droin, and M. Pinkoski.** 2003. Activation-induced cell death in T cells. Immunol. Rev. **193:**70–81.
18. **Hausler, P., G. Papoff, A. Eramo, K. Reif, D. A. Cantrell, and G. Ruberti.** 1998. Protection of CD95-mediated apoptosis by activation of phosphatidylinositide 3-kinase and protein kinase B. Eur. J. Immunol. **28:**57–69.
19. **Holmstrom, T. H., S. C. Chow, I. Elo, E. T. Coffey, S. Orrenius, L. Sistonen, and J. E. Eriksson.** 1998. Suppression of Fas/APO-1-mediated apoptosis by mitogen-activated kinase signaling. J. Immunol. **160:**2626–2636.
20. **Holmstrom, T. H., I. Schmitz, T. S. Soderstrom, M. Poukkula, V. L. Johnson, S. C. Chow, P. H. Krammer, and J. E. Eriksson.** 2000. MAPK/ERK signaling in activated T cells inhibits CD95/Fas-mediated apoptosis downstream of DISC assembly. EMBO J. **19:**5418–5428.
21. **Jones, R. G., A. R. Elford, M. J. Parsons, L. Wu, C. M. Krawczyk, W. C. Yeh, R. Hakem, R. Rottapel, J. R. Woodgett, and P. S. Ohashi.** 2002. CD28-dependent activation of protein kinase B/Akt blocks Fas-mediated apoptosis by preventing death-inducing signaling complex assembly. J. Exp. Med. **196:**335–348.
22. **Kitsberg, D., E. Formstecher, M. Fauquet, M. Kubes, J. Cordier, B. Canton, G. Pan, M. Rolli, J. Glowinski, and H. Chneiweiss.** 1999. Knock-out of the neural death effector domain protein PEA-15 demonstrates that its expression protects astrocytes from TNFalpha-induced apoptosis. J. Neurosci. **19:**8244–8251.
23. **Kubes, M., J. Cordier, J. Glowinski, J. A. Girault, and H. Chneiweiss.** 1998. Endothelin induces a calcium-dependent phosphorylation of PEA-15 in intact astrocytes: identification of Ser104 and Ser116 phosphorylated, respectively, by protein kinase C and calcium/calmodulin kinase II in vitro. J. Neurochem. **71:**1307–1314.
24. **Lee, Y. J., Y. K. Song, J. J. Song, R. R. Siervo-Sassi, H. R. Kim, L. Li, D. R. Spitz, A. Lokshin, and J. H. Kim.** 2003. Reconstitution of galectin-3 alters glutathione content and potentiates TRAIL-induced cytotoxicity by dephosphorylation of Akt. Exp. Cell Res. **288:**21–34.
25. **Lois, C., E. J. Hong, S. Pease, E. J. Brown, and D. Baltimore.** 2002. Germline transmission and tissue-specific expression of transgenes delivered by lentiviral vectors. Science **295:**868–872.
26. **Parsons, R.** 2004. Human cancer, PTEN and the PI-3 kinase pathway. Semin. Cell Dev. Biol. **15:**171–176.
27. **Peacock, J. W., and F. R. Jirik.** 1999. TCR activation inhibits chemotaxis toward stromal cell-derived factor-1: evidence for reciprocal regulation between CXCR4 and the TCR. J. Immunol. **162:**215–223.
28. **Peter, M. E., and P. H. Krammer.** 2003. The CD95(APO-1/Fas) DISC and beyond. Cell Death Differ. **10:**26–35.
29. **Podsypanina, K., L. H. Ellenson, A. Nemes, J. Gu, M. Tamura, K. M. Yamada, C. Cordon-Cardo, G. Catoretti, P. E. Fisher, and R. Parsons.** 1999. Mutation of Pten/Mmac1 in mice causes neoplasia in multiple organ systems. Proc. Natl. Acad. Sci. USA **96:**1563–1568.
30. **Ramos, J. W.** 2005. Cancer research center hotline: PEA-15 phosphoprotein: a potential cancer drug target. Hawaii Med. J. **64:**77–80.
31. **Renganathan, H., H. Vaidyanathan, A. Knapinska, and J. W. Ramos.** 2005. Phosphorylation of PEA-15 switches its binding specificity from ERK/MAPK to FADD. Biochem. J. **390:**729–735.
32. **Roy, S., and D. W. Nicholson.** 2000. Cross-talk in cell death signaling. J. Exp. Med. **192:**F21–F25.
33. **Sakai, A., C. Thieblemont, A. Wellmann, E. S. Jaffe, and M. Raffeld.** 1998. PTEN gene alterations in lymphoid neoplasms. Blood **92:**3410–3415.
34. **Scaffidi, C., S. Fulda, A. Srinivasan, C. Friesen, F. Li, K. J. Tomaselli, K. M. Debatin, P. H. Krammer, and M. E. Peter.** 1998. Two CD95 (APO-1/Fas) signaling pathways. EMBO J. **17:**1675–1687.
35. **Scaffidi, C., P. H. Krammer, and M. E. Peter.** 1999. Isolation and analysis of components of CD95 (APO-1/Fas) death-inducing signaling complex. Methods **17:**287–291.
36. **Staunton, J. E., D. K. Slonim, H. A. Coller, P. Tamayo, M. J. Angelo, J. Park, U. Scherf, J. K. Lee, W. O. Reinhold, J. N. Weinstein, J. P. Mesirov, E. S. Lander, and T. R. Golub.** 2001. Chemosensitivity prediction by transcriptional profiling. Proc. Natl. Acad. Sci. USA **98:**10787–10792.
37. **Strasser, A., A. W. Harris, D. C. Huang, P. H. Krammer, and S. Cory.** 1995. Bcl-2 and Fas/APO-1 regulate distinct pathways to lymphocyte apoptosis. EMBO J. **14:**6136–6147.
38. **Strauss, G., I. Knape, I. Melzner, and K. M. Debatin.** 2003. Constitutive caspase activation and impaired death-inducing signaling complex formation in CD95-resistant, long-term activated, antigen-specific T cells. J. Immunol. **171:**1172–1182.
39. **Suhara, T., T. Mano, B. E. Oliveira, and K. Walsh.** 2001. Phosphatidylinositol 3-kinase/Akt signaling controls endothelial cell sensitivity to Fas-mediated apoptosis via regulation of FLICE-inhibitory protein (FLIP). Circ. Res. **89:**13–19.
40. **Suzuki, A., M. Hayashida, H. Kawano, K. Sugimoto, T. Nakano, and K. Shiraki.** 2000. Hepatocyte growth factor promotes cell survival from Fas-mediated cell death in hepatocellular carcinoma cells via Akt activation and Fas-death-inducing signaling complex suppression. Hepatology **32:**796–802.
41. **Tan, Y., H. Ruan, M. R. Demeter, and M. J. Comb.** 1999. p90(RSK) blocks Bad-mediated cell death via a protein kinase C-dependent pathway. J. Biol. Chem. **274:**34859–34867.
42. **Tourian, L., Jr., H. Zhao, and C. B. Srikant.** 2004. p38alpha, but not p38beta, inhibits the phosphorylation and presence of c-FLIPS in DISC to potentiate Fas-mediated caspase-8 activation and type I apoptotic signaling. J. Cell Sci. **117:**6459–6471.
43. **Trencia, A., A. Perfetti, A. Cassese, G. Vigliotta, C. Miele, F. Oriente, S. Santopietro, F. Giacco, G. Condorelli, P. Formisano, and F. Beguinot.** 2003. Protein kinase B/Akt binds and phosphorylates PED/PEA-15, stabilizing its antiapoptotic action. Mol. Cell. Biol. **23:**4511–4521.
44. **Vlahos, C. J., W. F. Matter, K. Y. Hui, and R. F. Brown.** 1994. A specific inhibitor of phosphatidylinositol 3-kinase, 2-(4-morpholinyl)-8-phenyl-4H-1-benzopyran-4-one (LY294002). J. Biol. Chem. **269:**5241–5248.
45. **Wu, X., K. Senechal, M. S. Neshat, Y. E. Whang, and C. L. Sawyers.** 1998. The PTEN/MMAC1 tumor suppressor phosphatase functions as a negative regulator of the phosphoinositide 3-kinase/Akt pathway. Proc. Natl. Acad. Sci. USA **95:**15587–15591.
46. **Yang, B. F., C. Xiao, W. H. Roa, P. H. Krammer, and C. Hao.** 2003. Calcium/calmodulin-dependent protein kinase II regulation of c-FLIP expression and phosphorylation in modulation of Fas-mediated signaling in malignant glioma cells. J. Biol. Chem. **278:**7043–7050.
47. **Yin, X. M., K. Wang, A. Gross, Y. Zhao, S. Zinkel, B. Klocke, K. A. Roth, and S. J. Korsmeyer.** 1999. Bid-deficient mice are resistant to Fas-induced hepatocellular apoptosis. Nature **400:**886–891.
48. **Yuan, X. J., and Y. E. Whang.** 2002. PTEN sensitizes prostate cancer cells to death receptor-mediated and drug-induced apoptosis through a FADD-dependent pathway. Oncogene **21:**319–327.